Adherend surface morphology and its influence on the peel strength of adhesive joints bonded with modified phenolic and epoxy structural adhesives

J.P. Sargent

(British Aerospace, UK)

Received 15 June 1993; revised 14 October 1993

A detailed investigation of the interfacial region between the oxide and the adhesive/primer for aluminium peel test specimens, bonded with Redux 775 and AF163-2K/EC3960 and covering a range of peel strengths between about 1.8 to 12.3 N mm^{-1}, has been undertaken. Transmission electron microscopy (TEM) and scanning electron microscopy examination has shown that increasing adherend roughness on scales of tens of micrometres and tens of nanometres correlates with increasing peel strength. Measurements of carbon, aluminium and oxygen on both sides of the fracture surface for in situ *peeled AF163-2K specimens have been made using X-ray photoelectron spectroscopy. This was found to corroborate the TEM morphological evidence that enhanced peel strengths arise because of the presence of very fine scale whisker-like features at the surface of the oxide.*

Theoretical calculations are also presented which demonstrate one mechanism whereby roughness on a scale of tens of micrometres could give rise to enhanced peel strength.

Key words: adhesive/adherend interface; surface roughness; peel strength; oxide morphology; aluminium; modified phenolic; epoxy

Measurement of the peel strength of an adhesive joint is usually a very good way of ensuring that adequate quality control has been maintained in the manufacture of an adhesively bonded structure. The peel test is particularly sensitive to variations in a region adjacent to the interface between adhesive and adherend, and is widely used by the aerospace industry to ensure sufficient process control has been exercised during the pretreatment and anodizing of adherends. This sensitivity to interfacial quality has also been noted by, for example, Brockmann *et al.*[1].

Although peel strength is sensitive to interfacial quality, it is also affected to a greater or lesser extent by other physical variables of the adhesive joint; for example, adherend thickness or cohesive strength. For the purposes of process control this multiplicity of possible causes for peel strength variation can render it difficult to identify and correct problems in bond manufacture, and recourse sometimes has to be made to the physical examination of the whole range of variables within the adhesive joint by a variety of analytical methods. However, it is often possible to narrow down the range of likely causes for peel strength variation by careful inspection of the fracture paths, and decide, for example, whether fracture has occurred cohesively within the adhesive or primer, or adhesively between the oxide interface and the primer or adhesive.

0143-7496/94/01/0021–10

This paper reports on work conducted at the central research facility of British Aerospace (BAe) to identify some of those variables which, from fracture path investigation, indicated various amounts of adhesive failure.

Examination by scanning electron microscopy (SEM) was undertaken using a Cambridge 360, examination by transmission electron microscopy (TEM) using a Jeol 1200EX, and examination by X-ray photoelectron spectroscopy (XPS) using a VG Escalab MkII.

Specimens

All specimens prepared for examination were made from the intact ends of 25.4 mm wide peel specimens which remained after they had been pulled using a floating roller peel test (ASTM D3167-76). Peel specimens were bonded using both Redux 775, a commonly used phenolic-based system made by Ciba Composites comprising a phenolic resin and toughening polyvinyl formal (PVF) powder, and an epoxy adhesive AF163-2K and primer EC3960 made by 3M. All specimens used aluminium adherends (aluminium alloys 2014 and 2024) that had been subject to a nominally standard BAe processing route including degreasing, alkaline cleaning, grit-blasting, etching, chromic acid anodizing, rinsing and drying, priming and then bonding. Peel specimens were made using a thin upper adherend with a thickness of about 0.5 mm (the 'thin adherend') and a thicker lower adherend (the 'thick adherend') of about 1.5 mm. All peel strengths were derived from measurements using a floating roller test. Altogether, 19 Redux 775 specimens were selected from a larger archive containing many hundreds of specimens, and 14 AF163-2K specimens were selected, also from an archive containing many hundreds of specimens. These specimens were selected to be representative of specimens from the larger collections, covering the full range of peel strengths between about 1.8 and 12.3 N mm^{-1} for both resin systems.

SEM and TEM examination of Redux 775 specimens

In order to exclude the possibility that cohesive property variations were responsible for the measured range of peel strengths, a number of preliminary examinations were undertaken to screen all the specimens for deviations from a nominal adhesive and adherend thickness, and from obvious flaws and defects within the adhesive. No untoward deviations in thickness were found, and optical microscopy and SEM of sections of the adhesive revealed that no significant flaws or defects were present.

Optical examination of the fracture surfaces of the peel test specimens showed that specimens with lower peel strengths resulted in increasing amounts of failure adjacent to the thin adherend surface. This indicated that adherend surface examination would be productive, and an examination of the adherend surface topography was therefore undertaken. By first carefully polishing away the bulk of the adherends to leave a thin layer of aluminium on either side of the adhesive, and then dissolving the remainder of the adherend away using a mercuric chloride solution, it was possible to obtain replicas of the original surface structures. Fig. 1 shows examples of SEM images of the replica surface topography for specimens with a range of peel strengths. Although only six are shown here, it was noticeable that a distinct correlation between increasing peel strength and increasing surface roughness was apparent with all 19 specimens examined. SEM examination of the topography was also undertaken at a range of magnifications; this is shown in Fig. 2 for a specimen with a peel strength of 10.9 N mm^{-1} and shows evidence for a hierarchy of roughness scales.

In order to examine the very fine structure present at the interface between adherend and adhesive and examine some of the finer scale roughness like that seen in Fig. 2, it is necessary to use larger magnification. Remaining portions of peel test specimens were therefore prepared using an ultra-microtome to give cross-sections of aluminium, oxide and adhesive with thickness of about 100 nm, suitable for examination by TEM. These showed the characteristic columnar structure typical of the oxide when aluminium is chromic acid anodized, Fig. 3(a); the interfacial region between oxide and adhesive is shown at higher magnification in Fig. 3(b). However, examination of specimens with a range of peel strengths between 1.8 and 10.9 N mm^{-1} showed no correlation with any features of the oxide or interfacial region, other than the large, tens of micrometres scale, surface undulations observed above.

SEM and TEM examination of AF163-2K epoxy specimens

As before, optical and SEM screening of adhesive, adherend and primer for untoward deviations in nominal properties failed to show any property which could be correlated with peel strength. Instead, fracture path analysis indicated that the peel strength could be correlated with the varying degrees of failure which was apparently occurring at or adjacent to the adherend surface. Therefore, the adherend surface topography was examined using the same techniques as reported above for Redux 775. Replica adherend surfaces for specimens with a range of peel strengths from 1.2 to 12.3 N mm^{-1} were prepared and examined in the SEM. Although they showed similar sized (tens of micrometres) roughness features to those shown for the lower peel strength Redux 775 specimens above, no correlation with peel strength was observed.

The very fine structure at the interface present between adhesive primer and oxide was also examined using the TEM. Specimens were prepared in a similar manner to that described above, and Figs 4 and 5 show the adherend/primer interface for specimens with a low peel strength (2.1 N mm^{-1}) and a high peel strength (12.3 N mm^{-1}), respectively.

Figs 4(a) and 5(a) both show a primer layer at the top of the image, an oxide layer in the middle, and the underlying aluminium in the bottom of the images. The white regions in the primer regions are believed to be due to tearing of the primer around strontium chromate inclusions. The horizontal white bands in the aluminium, and the vertical dark lines running through the whole thickness of the oxide, are believed to be artefacts which originate from cutting when the specimen is microtomed.

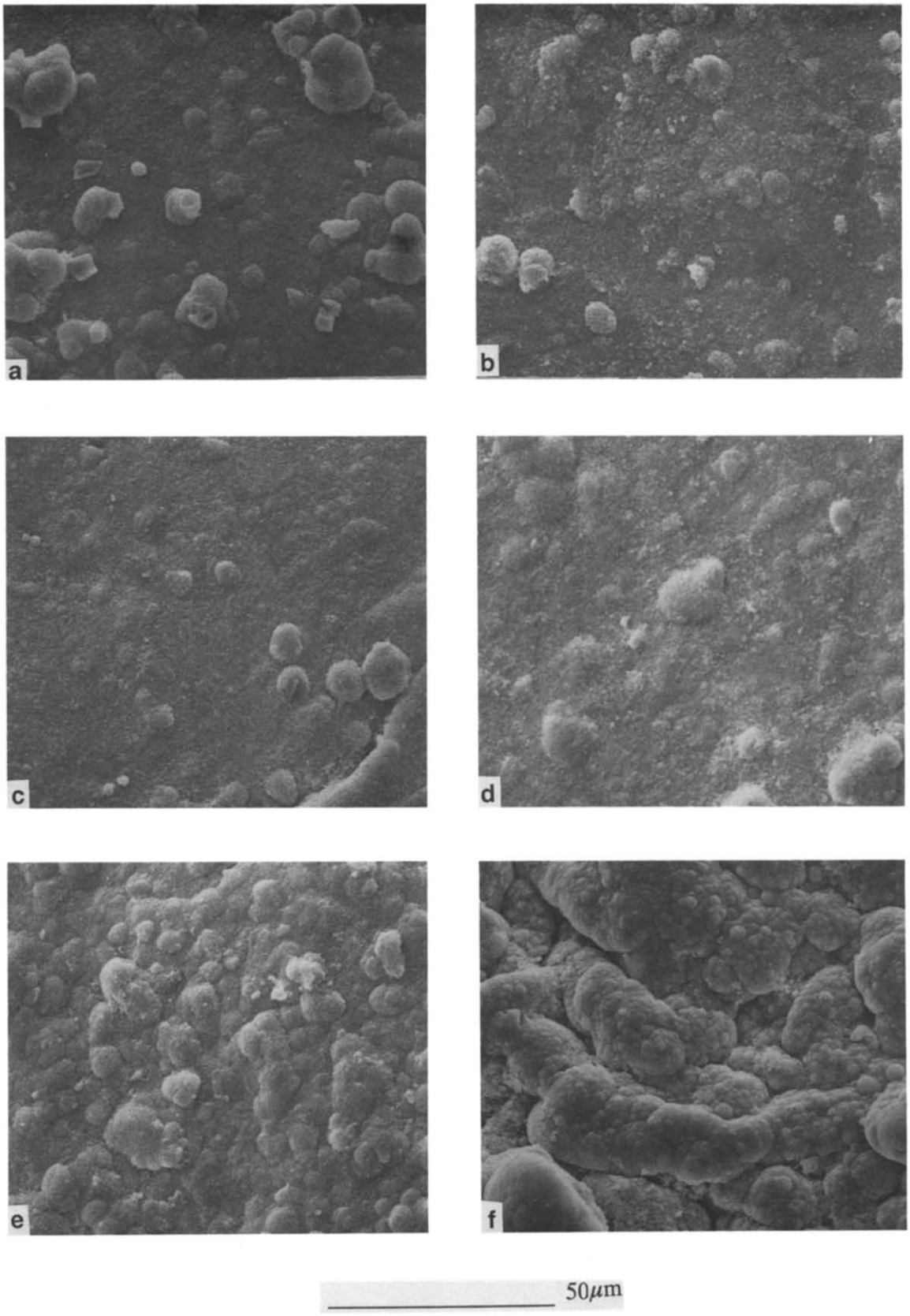

Fig. 1 SEM images of adherend replica surfaces for Redux 775. Specimen peel strength (N mm^{-1}): (a) 1.2; (b) 1.8; (c) 3.9; (d) 7.7; (e) 9.6; (f) 10.9

Both Figs 4 and 5 show images of oxide layers with a thickness of approximately 2 μm, and a branched, tree-like structure with increasingly fine detail towards the interface with the primer. At the highest magnification, it is apparent that a finer, more open oxide structure is present at the interface with primer for the high peel strength specimen (Fig. 5(b)) which is not present in the low peel strength specimen (Fig. 4(b)). The fine oxide structure in Fig. 5 appears to be made up of small whiskers, up to about 50 nm long, protruding into the primer region. Additionally, the whiskers seem to be well wetted with primer, and examination of the

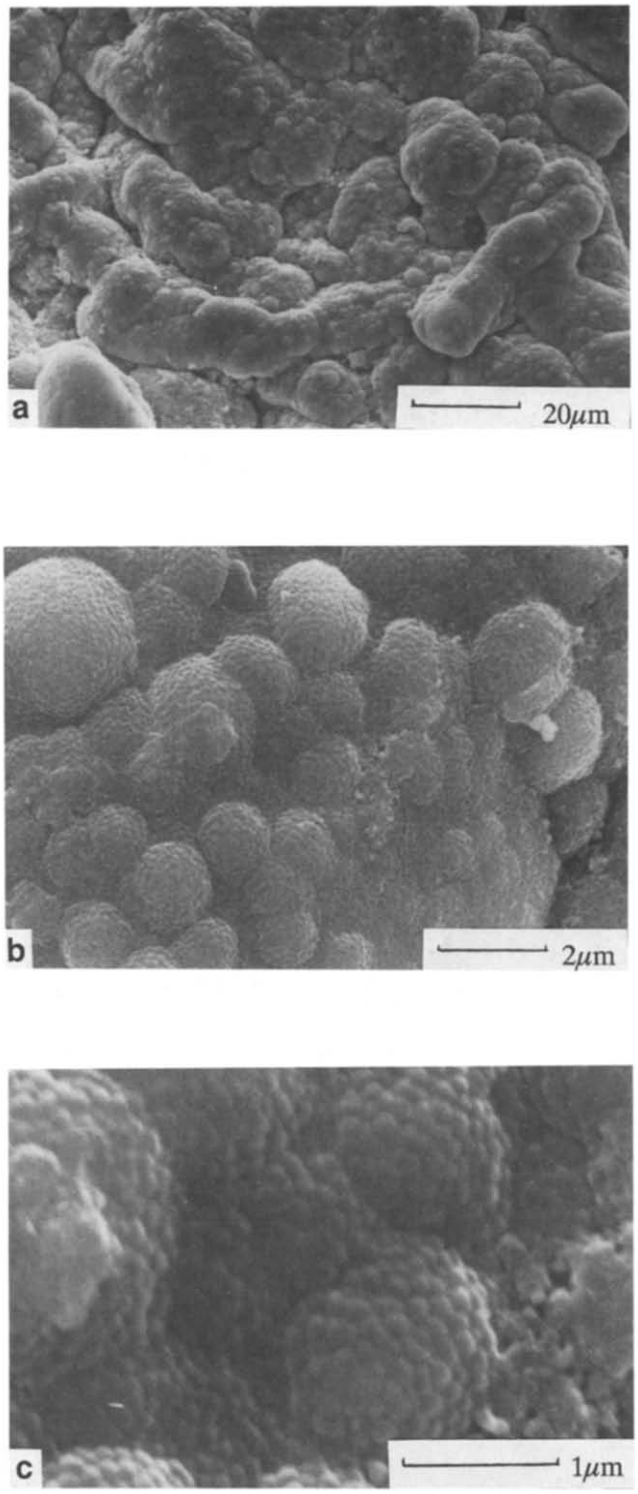

Fig. 2 SEM images of adherend replica surfaces for Redux 775 showing the hierarchy of roughness scales

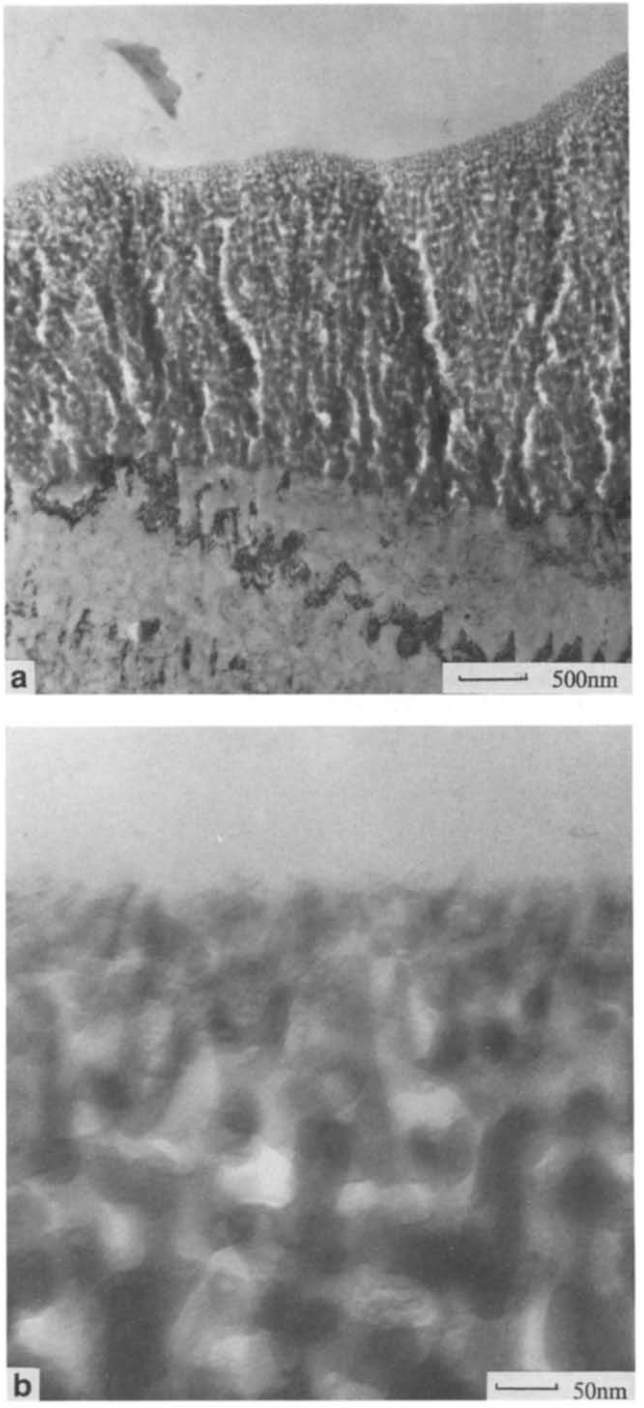

Fig. 3 (a) Cross-sectional TEM image of the interfacial region between adhesive Redux 775 (at the top of the image), oxide (in the middle) and aluminium adherend. (b) Cross-sectional high magnification TEM image of the interfacial region between adhesive Redux 775 (at the top of the image) and oxide (at the bottom)

photograph indicated primer extending several hundred nanometres down into the porous oxide layer.

The difference in fine-scale structure between the high and low peel strength specimens was sufficiently marked to warrant further examination of the interfacial region in other specimens. Fig. 6 shows a montage of photographs of the interfacial region for several specimens taken at the same magnification. Careful examination of the interfacial regions shows a pattern of gradually decreasing fine oxide structure correlating with declining peel strength.

XPS examination of AF163-2K specimens

Specimen preparation

To remove the risk of atmospheric contamination of freshly fractured surfaces, and obtain accurate chemical information in the interfacial region between oxide and primer, peeling of specimens prior to XPS examination was undertaken in an ultra-high vacuum using an *in situ* Tee-peeler. These were made from the same unpeeled ends of the AF163-2K peel test specimens used for TEM analysis above, and Fig. 7 shows an example of such a specimen. Detailed chemical depth

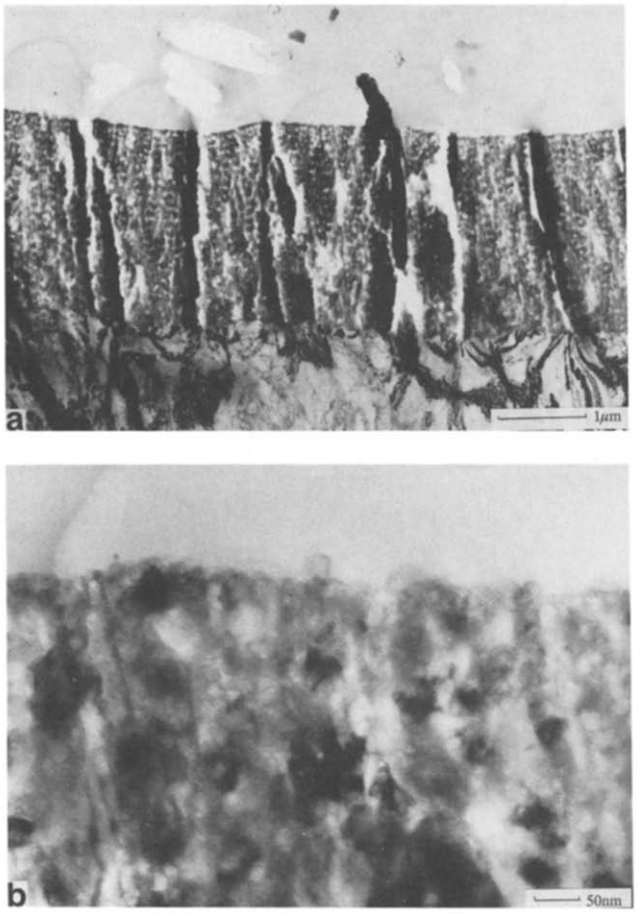

Fig. 4 (a) Cross-sectional TEM image of the interfacial region between adhesive/primer AF163-2K/EC3960 (at the top of the image), oxide (in the middle) and aluminium adherend for a low peel strength specimen (2.1 N mm^{-1}). (b) Cross-sectional high magnification TEM image of the interfacial region between adhesive/primer AF163-2K/EC3960 (at the top of the image) and oxide (at the bottom) for a specimen with low peel strength (2.1 N mm^{-1})

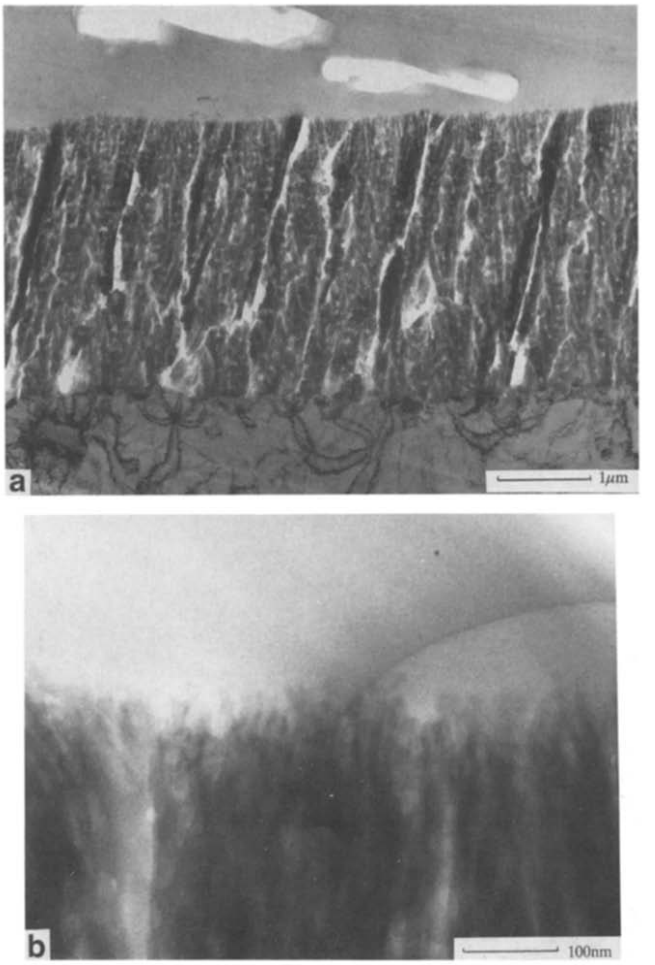

Fig. 5 (a) Cross-sectional TEM image of the interfacial region between adhesive/primer AF163-2K/EC3960 (at the top of the image), oxide (in the middle) and aluminium adherend for a high peel strength specimen (12.3 N mm^{-1}). (b) Cross-sectional high magnification TEM image of the interfacial region between adhesive/primer AF163-2K/EC3960 (at the top of the image) and oxide (at the bottom) for a specimen with high peel strength (12.3 N mm^{-1})

profiles about the primer and oxide in the interfacial region were obtained by repeatedly stripping away layers of material using argon ion bombardment, and then successively analysing the surfaces using XPS. Note that for polymeric materials ion bombardment results in graphitization, and surfaces comprising mostly adhesive, such as the thick adherend fracture surface, will incur increasing amounts of error in carbon/oxygen ratios as the depth profile proceeds. However, this effect will not be so marked on the thin adherend fracture surface, because the inorganic oxide is significantly more stable under the ion beam.

Results

Figs 8 and 9 shows SEM images of the thin adherend surfaces, after fracture in the ultra-high vacuum, of a large peel strength (10.7 N mm^{-1}) specimen and a low peel strength specimen (2.1 N mm^{-1}), respectively. At low and intermediate magnifications (Figs 8(a), 8(b) and 9(a), 9(b)), the surfaces show the characteristic rough (as a result of fragments of adhesive remaining on the adherend surface) and smooth surfaces indicating good and poor adhesive strength, respectively. The XPS technique samples a region which has an area of approximately 2 × 3 mm, and analysis of the large peel strength specimen was centred within the diamond pattern of the scrim cloth of the adhesive remaining on the adherend. However, since the analysis area is fairly broad, a check on the scrim cloth contribution to the signal was undertaken by restricting analysis to successively smaller areas within the diamond pattern using small-area XPS. This showed that restricting analysis to an area which did not include a contribution from the scrim cloth resulted in approximately 10% reduction in the carbon intensity, and approximately 5% increase in levels of aluminium and oxygen. It was also apparent from Fig. 8(b) that because of the good adhesion between primer and adherend, a small proportion of the XPS signal originating from the thin adherend fracture surface was inevitably made up of signals from pieces of adhesive and primer still adhering to the surface. By measuring the surface area which these covered, it was possible to estimate that approximately 15% of the signal intensity which originated from the large peel strength, thin adherend fracture surface was from adhesive/primer particles.

Figs 10 and 11 show carbon, oxygen, nitrogen and aluminium profiles on both sides of the fracture surface for a large peel strength (10.7 N mm^{-1}) and a low peel strength (2.1 N mm^{-1}) specimen, respectively. Carbon

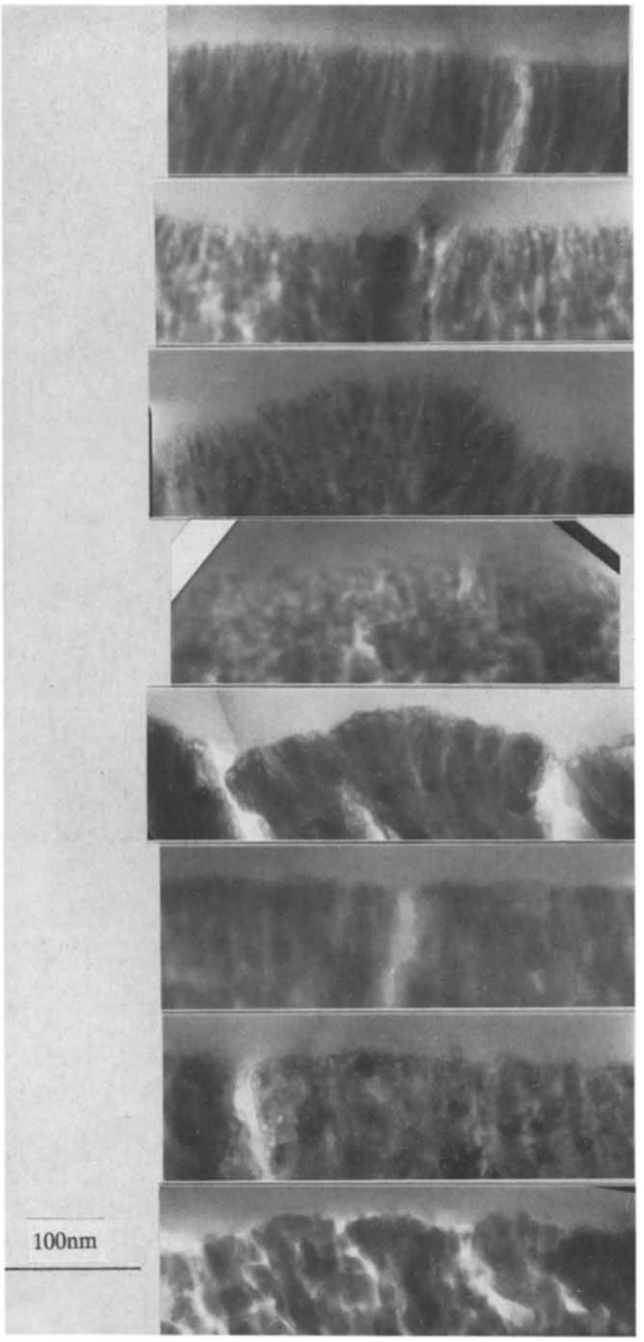

Fig. 6 Montage of TEM photographs showing cross-sections of the interface between primer and oxide surface. This shows the gradually increasing fine oxide surface structure as the peel strength increases. Specimen peel strength (N mm $^{-1}$), from top to bottom: 14.5; 13.5; 11.6; 9.5; 5.4; 4.9; 2.1; 1.9

can be used as an indicator of the presence of primer or adhesive, oxygen and aluminium indicates the presence of aluminium oxide, and nitrogen can indicate the presence of amine curing agents. Examination of the decline in carbon and increase in oxygen and aluminium levels on both fracture faces shows that fracture occurred within a few nanometres of the original interface between primer and aluminium oxide, for both high and low peel strength specimens.

In spite of the additional contribution from primer/adhesive particles and the scrim cloth, carbon levels on the thin adherend fracture surfaces declined to significantly lower levels for the low peel strength specimen (Fig. 11) than for the large peel strength

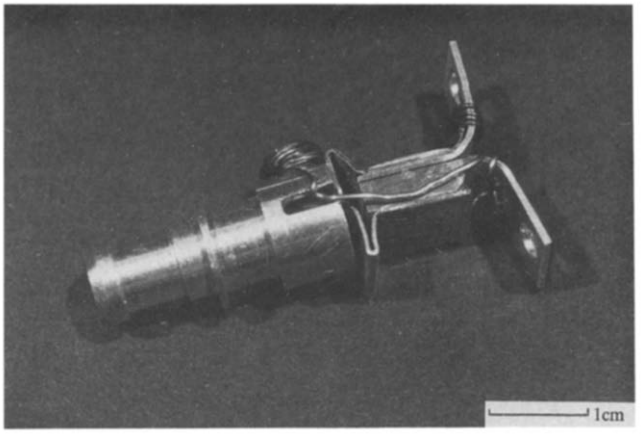

Fig. 7 Photograph of the small *in situ* peel test specimen and holder used for XPS analysis

specimen (Fig. 10). At the same time, oxygen levels increased to larger levels for the low peel strength specimen than for the large peel strength specimen. This indicated that, to a depth of at least 40 nm, a greater proportion of primer was present within the oxide layer for the large peel strength specimen than for the low peel strength specimen. This pattern is consistent with the TEM images of the interface shown above, where the large peel strength specimens had a more open micro-fibrous structure, permitting greater penetration of primer into the oxide layer and consequently leading to more gradual changes in oxygen and carbon. This contrasted with the low peel strength specimens, which had a much more closed surface oxide structure with a more abrupt change in interface between primer and oxide, leading to a greater change in oxygen and carbon levels at the fracture surfaces. Careful examination of both Figs 10 and 11 also reveals that there is evidence for a small increase in the nitrogen levels in the neighbourhood of the fracture surface.

In addition to recording the larger intensities of the major elements present in the neighbourhood of the fracture surface, measurements were also made of the lower intensity elements such as sodium, chromium, calcium, magnesium, etc. Figs 12 and 13 show the recorded intensity profiles for these elements for the same specimens shown in Figs 10 and 11 above, with a large peel strength (10.7 N mm $^{-1}$) and a low peel strength (2.1 N mm $^{-1}$), respectively. Although there seemed to be a concentration of various different elements at the interface, no correlation was observed between any particular element and the peel strength.

Discussion

Evidence has been presented here which demonstrates good correlation of peel strength with microstructural features of the primer/oxide interface. In particular, for Redux 775, increased oxide roughness on a scale of tens of micrometres, probably resulting from etching and grit-blasting, gave rise to increased levels of peel strength. In addition, evidence from both TEM and XPS showed that for AF163-2K/EC3960, an increase in the amount of an open, nanometre-sized micro-fibrous oxide layer between primer and oxide also resulted in increased levels of peel strength.

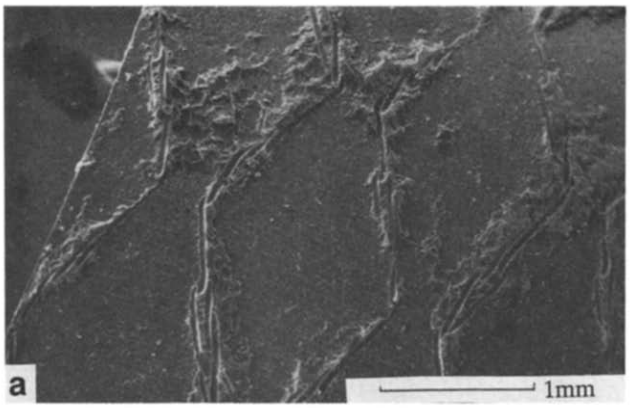

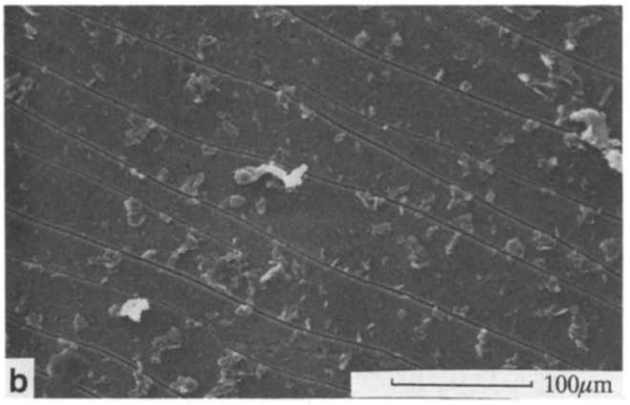

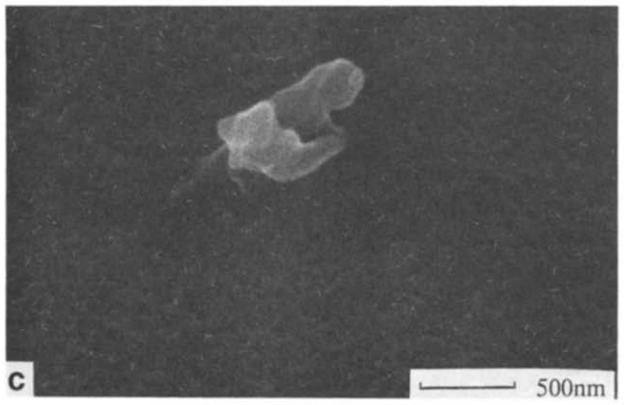

Fig. 8 SEM images of the thin adherend side of the *in situ* peel test specimen (peel strength = 10.7 N mm^{-1}) after peeling. Note in (a) the diamond pattern of scrim cloth; in (b) the small particles of adhesive/primer remaining on the surface and the long near-horizontal cracks in the oxide formed as a result of the bending of the thin adherend; in (c) a small particle of adhesive/primer adhering to the surface

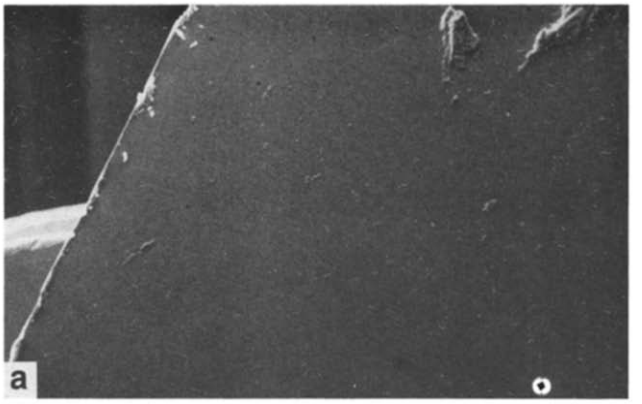

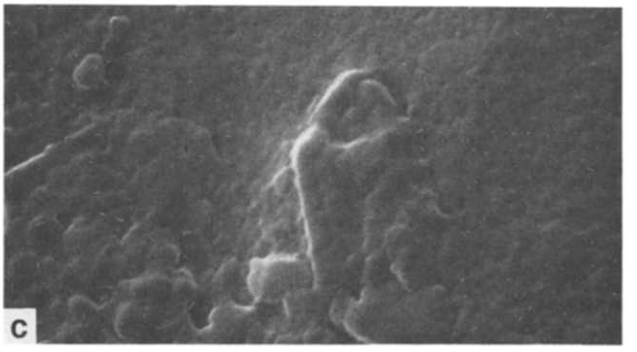

Fig. 9 SEM images of the thin adherend side of the *in situ* peel test specimen (peel strength = 2.1 N mm^{-1}) after peeling. Note the smooth adherend surfaces in (a) and (b). Magnifications as in Fig. 8

The influence of adherend surface roughness on a scale of nanometres has been noted by several authors to influence the peel strength. Bijlmer[2] found that fine etch pit structure within coarser etch pits was the most desirable structure for large peel strengths. Similar observations have also been made by Venables *et al.*[3], who used very high magnification scanning tunnelling electron microscopy to demonstrate that using an FPL etch generated a surface with fine oxide protrusions, similar in appearance to those seen here, which were sufficient to increase peel adhesion by a factor of 10. The importance of the interfacial region, and the influence of the very fine structure in determining adhesive bond strength, has also been recognized by other workers. For example, Bishopp[4] observed that with some primers, poor wetting of the very fine oxide structure led to reductions in peel strength.

It is worthwhile considering in more detail how roughness on a scale of tens of micrometres, like that seen here for Redux 775 specimens, contributes to peel strength. Possible contributions to peel strength as a result of roughness on this scale could act via alterations in the microscopic stress distribution adjacent to etch pits, giving rise to stress concentrations and sites for crack propagation in the adhesive, and the physical impediment of the crack path running adjacent to the adherend surface. A further contribution to peel strength would also arise simply because of the additional normal force required to remove adhesive from an adherend surface because of the increased surface area and departure of the adherend surface from flatness.

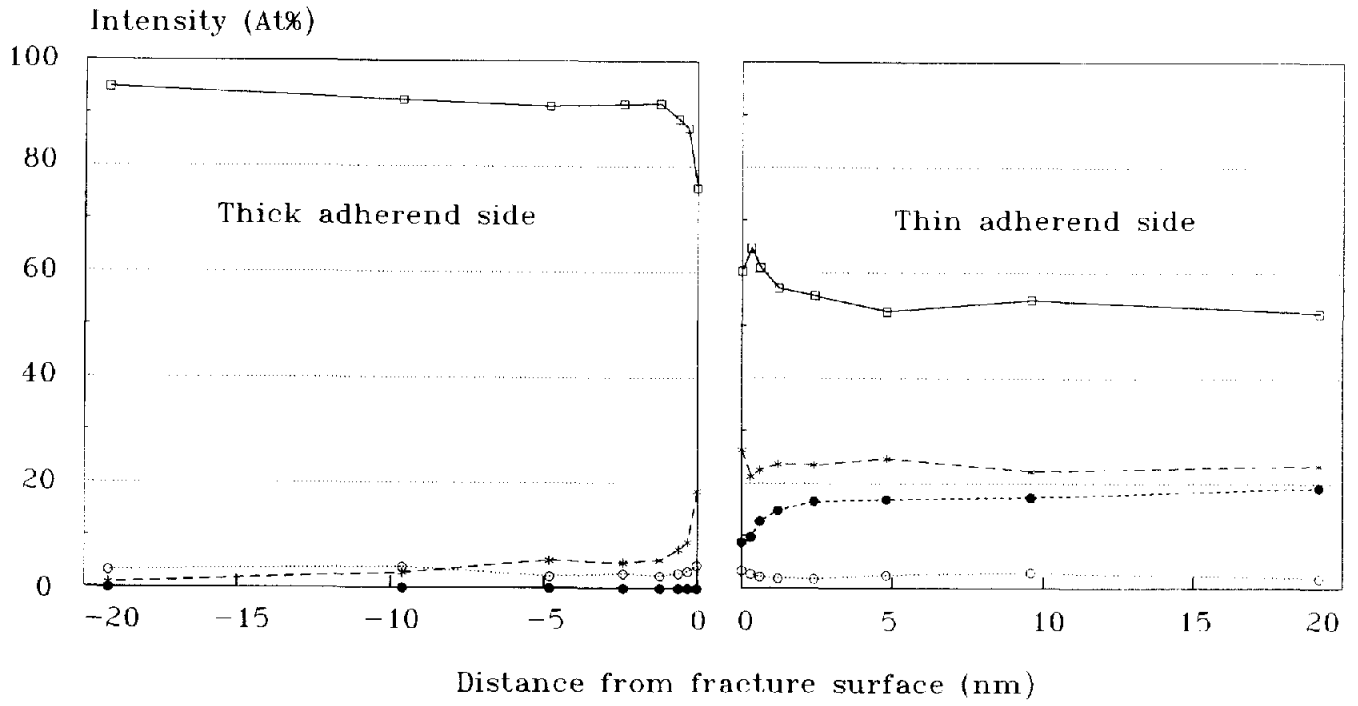

Fig. 10 XPS intensities of carbon (— □ —), oxygen (— — * — —), aluminium (- - - ● - - -) and nitrogen (··· ○ ···) as a function of depth into both sides of the adherend fracture surfaces. Large peel strength specimen, peel strength = 10.7 N mm^{-1}

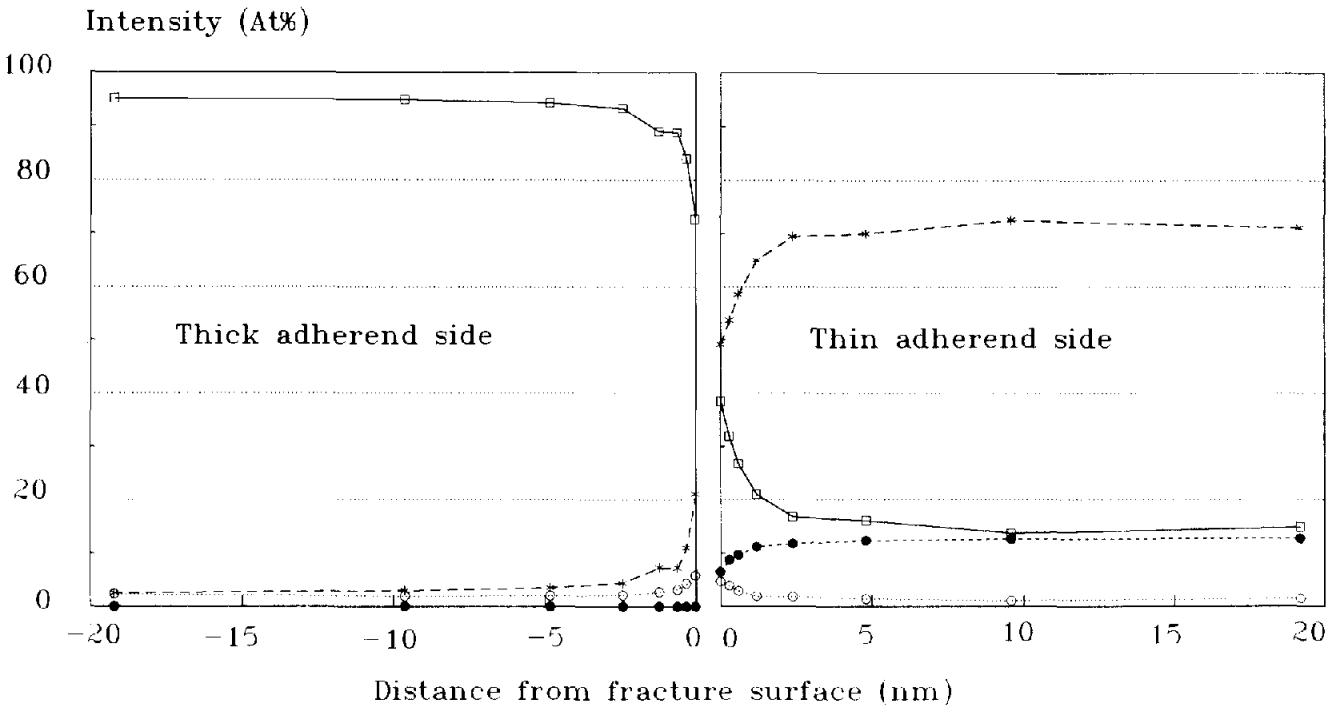

Fig. 11 XPS intensities of carbon (— □ —), oxygen (— — * — —), aluminium (- - - ● - - -) and nitrogen (··· ○ ···) as a function of depth into both sides of the adherend fracture surfaces. Low peel strength specimen, peel strength = 2.1 N mm^{-1}

It is possible to analyse the expected contribution from increased area and departures from flatness by considering the force distribution at an idealized surface composed of spherical depressions. Crocombe and Adams[5] demonstrated that in a peel test the principal tensile stress, which acts with a large normal component, drives the crack towards the thinner, flexible adherend.

Given that a normal force (F) is required to cause an intrinsic adhesive failure at a smooth flat surface, then a larger force (G) is required for a rough surface composed of valleys and pits because of the increased effective surface area. In addition, the magnitude of this force will be proportionately greater as the angle it makes with a normal to the surface increases. It is a relatively simple matter to examine the forces required to detach a unit area of adhesive from a surface, given deviations from flatness.

Consider an idealized valley of an adherend surface in the form of a spherical depression, Fig. 14. If f is the

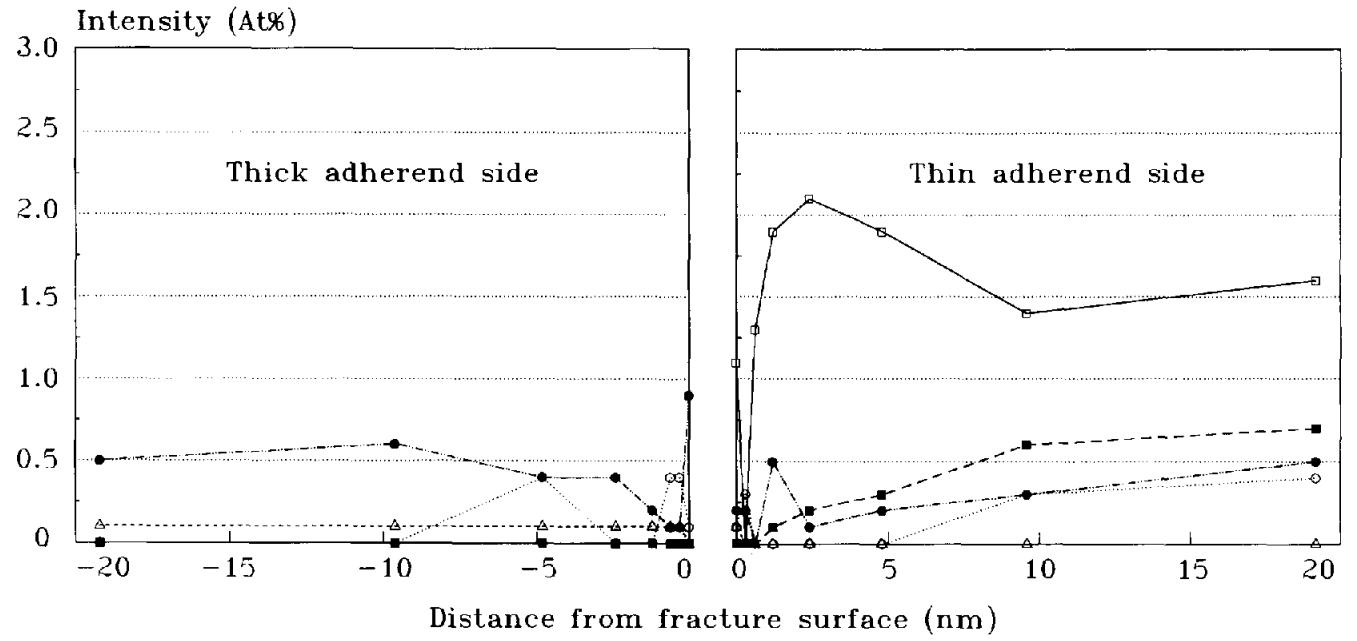

Fig. 12 XPS intensities of the minor elements (— □ —, Si; - - - △ - - -, Sr; ··· ○ ···, Cr; — — ■ — —, Cu; — · · — ● — · · —, Br) as a function of depth into both sides of the adherend fracture surfaces. Large peel strength specimen, peel strength = 10.7 N mm^{-1}

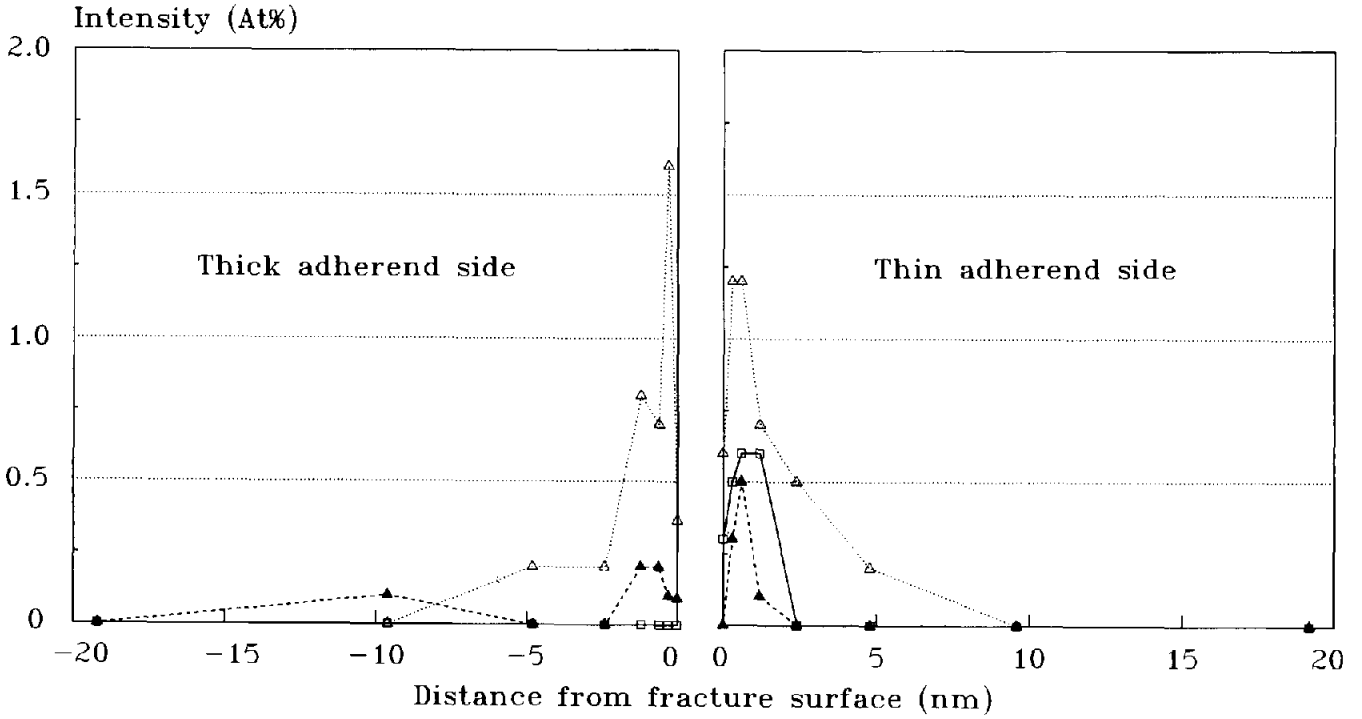

Fig. 13 XPS intensities of the minor elements (— □ —, Ca; - - - ▲ - - -, Mg; ··· △ ···, Na) as a function of depth into both sides of the adherend fracture surfaces. Low peel strength specimen, peel strength = 2.1 N mm^{-1}

normal force required to detach unit area of adhesive and g is the equivalent force at an angle θ required to detach unit area of adhesive, then, from Fig. 14:

$$g = f/\cos\theta$$

and area of element of sphere is given by:

$$\delta A = r\delta\theta \times l\delta\phi$$

Since:

$$l = r\sin\theta$$

then:

$$\delta A = r\delta\theta \times r\sin\theta\delta\phi$$

Therefore the total area is given by:

$$A = \int_0^{\pi} d\phi \int_{\theta}^{-\theta} r\mathrm{d}\theta \times r\sin\theta$$

Therefore the total force is:

$$G = \int_0^{\pi} \mathrm{d}\phi \int_{\theta}^{-\theta} fr^2 \frac{\sin\theta}{\cos\theta}\,\mathrm{d}\theta$$

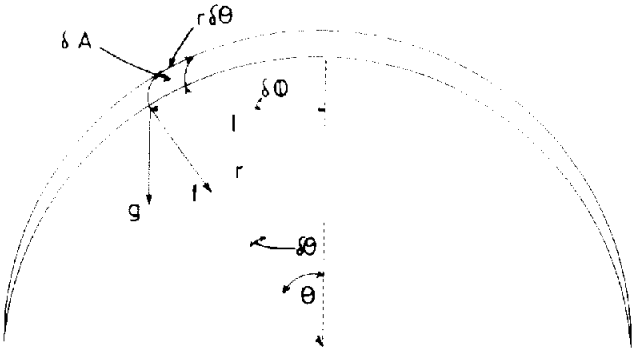

Fig. 14 Diagram showing part of an idealized spherical depression, defining the parameters used in the analysis to derive the equivalent forces required to detach adhesive from a surface

$$= fr^2 \int_0^{\pi} d\phi \int_0^{\theta} \tan\theta \, d\theta$$

$$= fr^2 \pi \left[\log \sec\theta\right]_0^{\theta} \quad (1)$$

Then, by substitution of suitable values for θ into the above expression, the integral can be evaluated. For example, Fig. 15 shows the edge-on SEM image for the replica surface of a specimen with a peel strength of 5.3 N mm^{-1}, in the region of an etch pit. This gives an angle for θ of approximately 30°.

From Equation (1) above:

$$G = \pi r^2 f \times 0.288$$

For an equivalent, smooth flat surface it is easily shown that the normal force F to detach adhesive from the same subtended surface area is:

$$F = \pi r^2 f \times 0.25$$

Comparing F and G, it is seen that a valley with this geometry gives an increase in force required to detach adhesive of 15% over that for the flat smooth surface.

Similar examples can also be calculated for valleys with angles of 45° and 60°. These give increases in the force required to detach adhesive, over that for the flat smooth surfaces, of 39% and 85%, respectively.

Surfaces like that shown in Fig. 1 for a large peel strength specimen, when compared with the surfaces for a low peel strength specimen, also in Fig. 1, are very rough indeed. In the light of the analysis outlined above, such rough surfaces could probably be considered to be made up of depressions with angles greater than 60°. This would result in a consequent net increase in force required to detach adhesive considerably in excess of the value of 85%. It is not unrealistic to consider that although the net increase in force, or equivalently peel force, would eventually be limited by the cohesive strength of the adhesive or primer, it would nevertheless permit a much greater latitude in the intrinsic adhesive bond strength requirements necessary to fulfil a minimum peel strength.

Conclusions

SEM examination of the adherend surface structure of peel test specimens bonded with Redux 775 has shown good correlation of adherend surface roughness on a scale of tens of micrometres with peel strength.

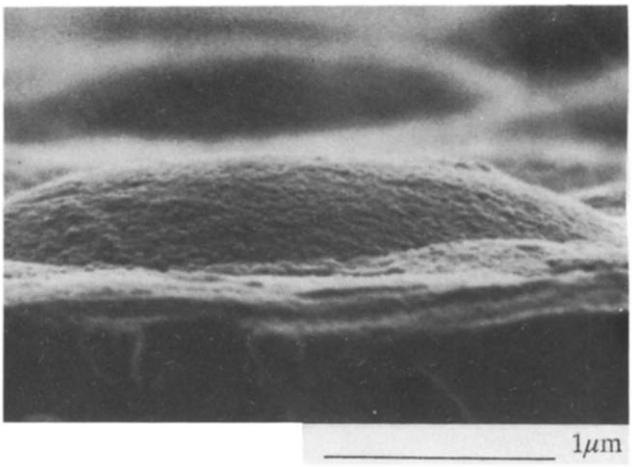

Fig. 15 SEM image of the replica surface of an etch pit for a specimen of AF163-2K/EC3960 and with a peel strength of 5.3 N mm^{-1}. Angle θ of about 30°

TEM and XPS investigation of the interfacial region between AF163-2K/EC3960 and the surface of aluminium adherends showed a good correlation of peel strength with the very fine, nanometre-sized structures at the surface of the oxide.

Theoretical calculations are also presented which corroborate the experimental results, suggesting that one mechanism where peel strength can be influenced is via adherend roughness on a scale of a few tens of micrometres.

Acknowledgements

The author would like to thank Dr S.J. Harris, of the Sowerby Research Centre, for his results and assistance with the interpretation of the XPS work, and for his helpful comments on this manuscript. The author also thanks Mr P. Harrison, of Airbus, BAe Filton, Bristol, UK, for supplying the specimens and peel strength results.

References

1 **Brockmann, W., Hennemann, O.-D., Kollek, H. and Matz, C.** 'Adhesion in bonded aluminium joints for aircraft construction' *Int J Adhesion and Adhesives* **6** No 3 (1986) p 115

2 **Bijlmer, P.F.A.** 'Influence of chemical pretreatments on surface morphology and bondability of aluminium' *J Adhesion* **5** (1973) p 319

3 **Venables, J.D., McNamara, D.K., Chen, J.M., Sun, T.S. and Hopping, R.L.** 'Oxide morphologies on aluminium prepared for adhesive bonding' in *'Applications of Surface Science', Vol 3* (North Holland Publishing Company, 1979) p 88

4 **Bishopp, J.A.** 'Novel surface and interfacial analysis techniques as aids to the development of new, high fracture toughness film adhesives' *Int J Adhesion and Adhesives* **4** (1984) p 153

5 **Crocombe, A.D. and Adams, R.D.** 'Peel analysis using the finite element method' *J Adhesion* **12** (1981) p 127

Author

The author is with the Sowerby Research Centre, British Aerospace, Bristol, UK.